



## Azole-based inhibitors of AKT/PKB for the treatment of cancer

Qingping Zeng<sup>a</sup>, John G. Allen<sup>a,\*</sup>, Matthew P. Bourbeau<sup>a</sup>, Xianghong Wang<sup>a</sup>, Guomin Yao<sup>a</sup>, Seifu Tadesse<sup>a</sup>, James T. Rider<sup>a</sup>, Chester C. Yuan<sup>a</sup>, Fang-Tsao Hong<sup>a</sup>, Matthew R. Lee<sup>a</sup>, Shiwen Zhang<sup>b</sup>, Julie A. Lofgren<sup>b</sup>, Daniel J. Freeman<sup>b</sup>, Suijin Yang<sup>b</sup>, Chun Li<sup>c</sup>, Elizabeth Tominey<sup>c</sup>, Xin Huang<sup>d</sup>, Douglas Hoffman<sup>e</sup>, Harvey K. Yamane<sup>f</sup>, Christopher Fotsch<sup>a</sup>, Celia Dominguez<sup>a</sup>, Randall Hungate<sup>a</sup>, Xiaoling Zhang<sup>b</sup>

<sup>a</sup> Chemistry Research and Discovery, Amgen Inc., One Amgen Center Drive, Thousand Oaks, CA 91320, United States

<sup>b</sup> Oncology Research, Amgen Inc., One Amgen Center Drive, Thousand Oaks, CA 91320, United States

<sup>c</sup> Pharmacokinetics and Drug Metabolism, Amgen Inc., One Amgen Center Drive, Thousand Oaks, CA 91320, United States

<sup>d</sup> Chemistry Research and Discovery, Amgen, Inc., 360 Binney St., Cambridge, MA 02142, United States

<sup>e</sup> Small Molecule Process and Product Development, Amgen Inc., One Amgen Center Drive, Thousand Oaks, CA 91320, United States

<sup>f</sup> Protein Science, Amgen Inc., One Amgen Center Drive, Thousand Oaks, CA 91320, United States

### ARTICLE INFO

#### Article history:

Received 19 December 2009

Revised 9 January 2010

Accepted 13 January 2010

Available online 21 January 2010

#### Keywords:

PKB

AKT

Cancer

SAR studies

### ABSTRACT

Through a combination of screening and structure-based rational design, we have discovered a series of *N*<sup>1</sup>-(5-(heterocyclyl)-thiazol-2-yl)-3-(4-trifluoromethylphenyl)-1,2-propanediamines that were developed into potent ATP competitive inhibitors of AKT. Studies of linker strand-binding adenine isosteres identified SAR trends in potency and selectivity that were consistent with binding interactions observed in structures of the inhibitors bound to AKT1 and to the counter-screening target PKA. One compound was shown to have acceptable pharmacokinetic properties and to be a potent inhibitor of AKT signaling and of *in vivo* xenograft tumor growth in a preclinical model of glioblastoma.

© 2010 Elsevier Ltd. All rights reserved.

A serine/threonine kinase with three isoforms, AKT (protein kinase B, PKB) is a key enzyme in the phosphatidylinositol-3-kinase (PI3K) pathway, and is involved in signaling by multiple growth factors. Gain-of-function mutations of PI3K<sup>1,2</sup> and AKT,<sup>3</sup> loss-of-function mutations of the tumor suppressor phosphatase and tensin homolog (PTEN),<sup>4</sup> and amplification of human epidermal growth factor receptor 2 (HER2)<sup>5</sup> have been shown to confer constitutive AKT activity. Genetic events leading to aberrant AKT activity represent one of the most common molecular mechanisms associated with human cancers.<sup>6</sup> These data taken together support the hypothesis that AKT inhibitors may be useful for the treatment of cancer.

Several research groups<sup>7</sup> have developed AKT inhibitors including GSK2141795 entering phase I clinical trials, and allosteric inhibitor MK-2206 that has completed phase I trials.<sup>8</sup> In the preceding Letter<sup>9</sup> we discussed the discovery and optimization of a series of thiadiazole-based AKT inhibitors (i.e., **1**, Fig. 1). Herein we describe SAR studies of the azole ring that lead to the identification of the thiazole series (**2**). By varying the substituent at the 5 position of the thiazole in **2** (Ar, linker binder), interactions with

Glu228-Ala230 (the linker strand connecting the C- and N-terminal domains of AKT1) were explored. Potency was evaluated by biochemical inhibition of AKT1 and inhibition of phosphorylation of proline-rich AKT substrate 40 (PRAS40) in U-87 MG cells.<sup>9,10</sup> Selectivity screening against protein kinase A (PKA), a close structural homolog of AKT, was expected to lead to broader kinase selectivity. In parallel, screening for selectivity against cyclin-dependent kinase 2 (CDK2), a kinase essential for cell proliferation, was expected to result in a reduction of off-target effects in *in vivo* tumor xenograft studies.

Azole ring analogs were prepared by the convergent routes outlined in Scheme 1. The 4-trifluoromethylphenyl sidechain was

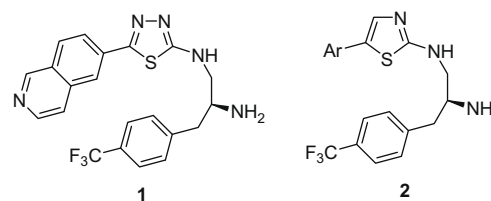
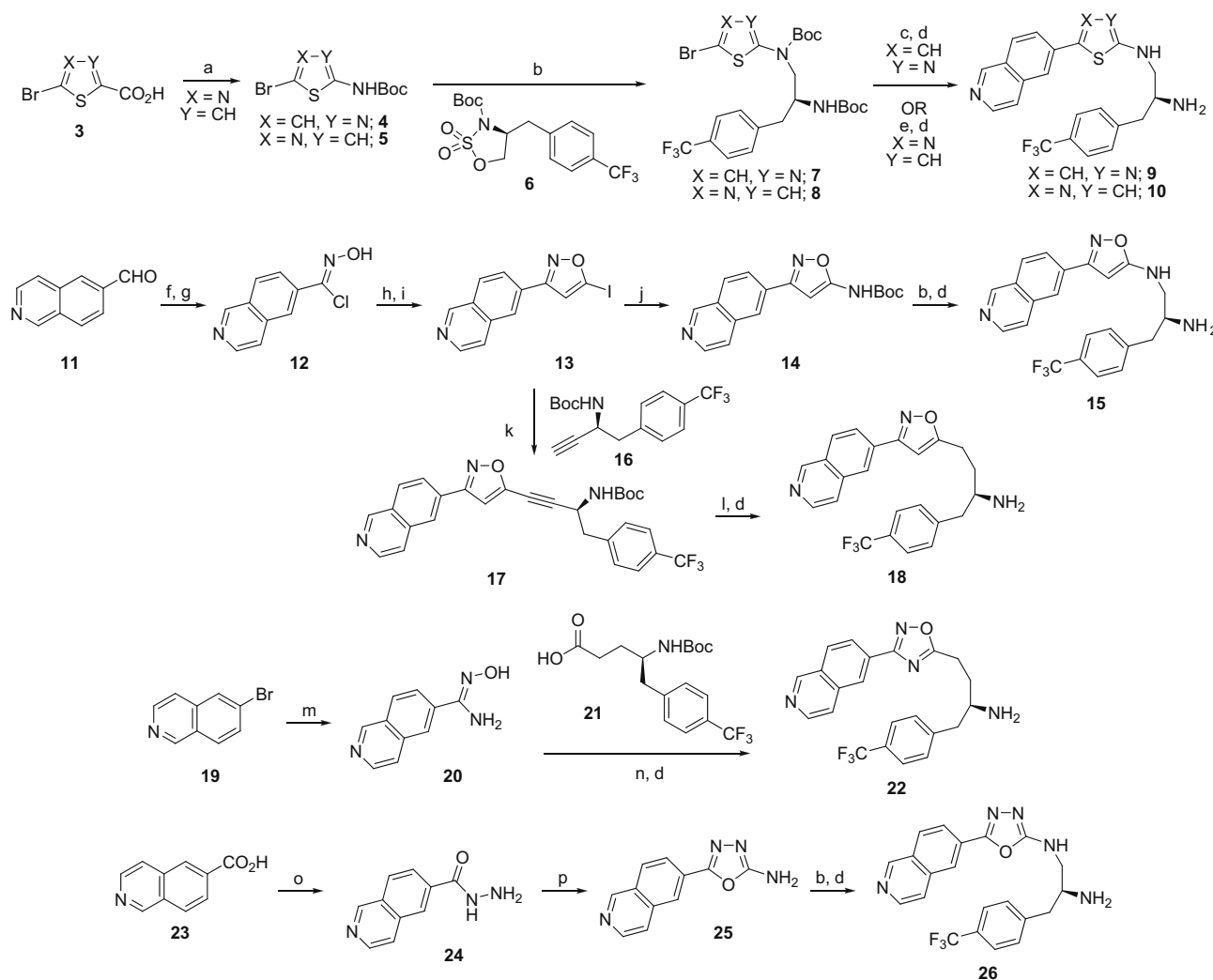


**Figure 1.** Thiadiazole-based AKT inhibitor **1** and thiazole-based AKT inhibitor of type **2**.

\* Corresponding author. Tel.: +1 805 313 5257.

E-mail address: [johallen@amgen.com](mailto:johallen@amgen.com) (J.G. Allen).



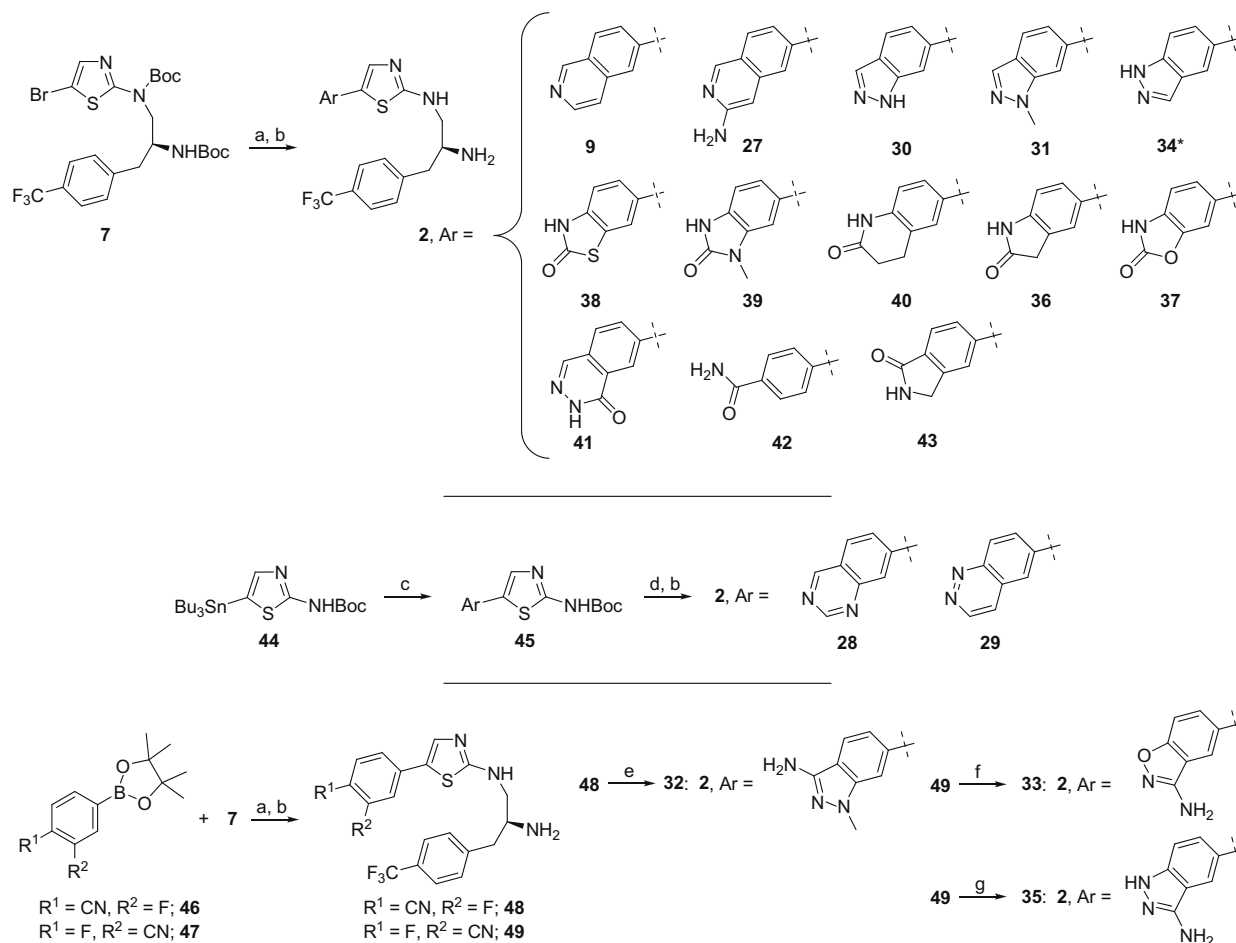
**Scheme 1.** Reagents and conditions: (a) diphenylphosphorylazide, Et<sub>3</sub>N, *t*-BuOH, 80 °C, 66%; (b) *tert*-butyl (4*S*)-4-(4-(trifluoromethyl)benzyl)-1,2,3-oxathiazolidine-3-carboxylate 2,2-dioxide (**6**), Cs<sub>2</sub>CO<sub>3</sub>, DMF, 50 °C, 20–92%; (c) isoquinolin-6-ylboronic acid, tetrakis(triphenylphosphine)palladium, Na<sub>2</sub>CO<sub>3</sub>, dioxane, water, 90 °C, 74%; (d) TFA, CH<sub>2</sub>Cl<sub>2</sub>, rt, 63–93%; (e) isoquinolin-6-ylboronic acid, bis(di-*t*-butylphenylphosphine)palladium dichloride, KOAc, acetonitrile, water, 100 °C, 4%; (f) hydroxylamine HCl, EtOH, water, 50% NaOH, 0 °C, 84%; (g) NCS, DMF, 0–50 °C, 91%; (h) tributyl(ethynyl)stannane, Et<sub>3</sub>N, THF, 0 °C to rt, 47%; (i) iodine, THF, 80 °C, 78%; (j) *t*-butylcarbamate, X-Phos, Pd<sub>2</sub>dba<sub>3</sub>, Cs<sub>2</sub>CO<sub>3</sub>, dioxane, 120 °C, 41%; (k) (*S*)-*tert*-butyl 1-(4-(trifluoromethyl)phenyl)but-3-yn-2-ylcarbamate (**16**), bis(triphenylphosphine)palladium dichloride, copper(I)iodide, Et<sub>3</sub>N, 65 °C, 51%; (l) Pd–C, H<sub>2</sub>, MeOH, rt, 89%; (m) (i) CuCN, NMP, 150–170 °C; (ii) hydroxylamine HCl, MeOH, Na<sub>2</sub>CO<sub>3</sub>, rt to 50 °C, 9%; (n) (*R*)-4-(*tert*-butoxycarbonyl)-5-(4-(trifluoromethyl)phenyl)pentanoic acid (**21**), CDI, DMF, 100 °C, 31%; (o) CDI, hydrazine, rt, 69%; (p) (i) BrCN, imidazole, CH<sub>2</sub>Cl<sub>2</sub>, reflux; (ii) hydrazine, THF, reflux, 96%.

introduced as an amino acid derived building block by alkylation with 1,2,3-oxathiazolidine-3-carboxylate 2,2-dioxide **6**,<sup>11</sup> Sonogashira coupling with alkyne **16**<sup>12</sup> or condensation with  $\gamma$ -amino acid **21**.<sup>13</sup> Compounds **9** and **10** were prepared from intermediates **4** and **5** by sequential sidechain alkylation with **6**, Suzuki coupling<sup>14</sup> with isoquinoline boronic acid and finally deprotection with TFA. Isoxazole analog **15** was prepared from **14** and **6**. Isoxazole **18**, containing a 5-position methylene, was prepared from **13** by Sonogashira coupling with **16** followed by hydrogenation. The 1,2,4-oxadiazole ring of analog **22**, was assembled by condensing **21** with hydroxyacetimidamide **20**. The 1,3,4-oxadiazole ring in **26** was prepared by reacting isoquinoline-6-carbohydrazide **24** with di(1*H*-imidazol-1-yl)methanimine prepared in situ.

Thiazole compounds containing alternative linker binding elements were prepared as shown in Scheme 2. Suzuki couplings of **7** with aryl boronic acids or aryl pinacolboronates, prepared by lithium halogen exchange and quenching with triisopropylboronate or by Miyaura coupling of aryl bromides or chlorides with pinacol diborane,<sup>15</sup> provided a range of arylated thiazoles **2**. The

bis(di-*t*-butylphenylphosphine)palladium catalyst was particularly useful in the preparation of carbonyl-containing linker binders (**36–43**).<sup>11</sup> Stille couplings were used in cases where arylboronates were difficult to form (**28** and **29**). Compounds containing 3-aminoindazoles (**32** and **35**) and a 3-aminobenzisoxazole (**33**) could be prepared from the corresponding common late stage fluorobenzonitrile intermediates (**48** and **49**) by treatment with methylhydrazine, hydrazine or *N*-hydroxyacetamide in the presence of potassium *tert*-butoxide.

We initially explored the SAR around the core azole ring while keeping the isoquinoline linker binder element of the potent thiazole analog **19** constant (Table 1). As discussed in the previous Letter,<sup>9</sup> the thiazole series of compounds bound in a U-shaped conformation and formed a hydrogen bond with the sidechain of the catalytic Lys179 residue, and the 2-amino group formed an ionic interaction with Asp292 (AKT1 numbering as shown in Figure 2A). A similar Lys179 contact was made by thiazole **9**, but did not appear to be possible for isomeric thiazole **10**, explaining the observed loss of potency. Compounds **15**, **18**, and **22** also appeared



**Scheme 2.** Reagents and conditions: (a) arylboronic acid or arylpinacolboronate, bis(di-*t*-butylphenylphosphine)palladium dichloride or bis(triphenylphosphine)dichloride or tetrakis(triphenylphosphine)palladium,  $\text{Na}_2\text{CO}_3$  or KOAc, dioxane or acetonitrile or dimethoxyethane, water or water-ethanol, 85–150 °C, 8–89%; (b) TFA, or TFA- $\text{CH}_2\text{Cl}_2$ , rt, 38–89%; (c) arylbromide, tetrakis(triphenylphosphine)palladium, CsF-CuI or LiCl, DMF, 80–100 °C, 46–73%; (d) *tert*-butyl (4S)-4-(4-(trifluoromethyl)benzyl)-1,2,3-oxathiazolidine-3-carboxylate 2,2-dioxide,  $\text{Cs}_2\text{CO}_3$ , DMF, 50 °C, 33–96%; (e) methylhydrazine, 100 °C, 69%; (f) *N*-hydroxyacetamide, KOtBu, DMF, 20%; (g) hydrazine, 100 °C, 38–62%. \*Compound **34** was prepared with the corresponding 4-chlorophenyl side chain instead of the 4-trifluoromethylphenyl side chain.

**Table 1**

AKT, PKA and CDK2 enzyme inhibition and inhibition of PRAS40 phosphorylation (Thr246) in U-87 MG cells forazole core analogs<sup>a</sup>

Compd	AKT1 IC <sub>50</sub> (nM)	PKA IC <sub>50</sub> (nM)	CDK2 IC <sub>50</sub> (nM)	pPRAS40 IC <sub>50</sub> (μM)
<b>1</b> <sup>9</sup>	3.2 ± 0.9	7.6 ± 15	53 ± 23	0.25 ± 0.11
<b>9</b>	4.9 ± 3.6	5.9 ± 4.2	12.4 ± 5.7	0.43 ± 0.27
<b>10</b>	404 ± 31	187 ± 23	1070 ± 120	NT
<b>15</b>	17	40	93	NT
<b>18</b>	40 ± 18	50 ± 8.7	117 ± 30	3.8
<b>22</b>	1600 ± 230	980 ± 74	4630	NT
<b>26</b>	85 ± 12	133 ± 9.1	348 ± 100	NT

<sup>a</sup> Data is given as the mean ± standard deviation (SD) where three or more measurements were made. NT indicates not tested.

to be able to engage Lys179. However, the isoxazole core of **15** directed a hydrogen atom toward the sidechain phenyl ring and may have destabilized the U-shaped binding conformation of **15** compared to **1** or **9** (molecular mechanical modeling not shown). Isoxazole **18** had a methylene at the sidechain rather than a 5-amino *N*-linkage, and loss of interaction with Asp292 further decreased potency. The reduced potency of 1,2,4-oxadiazole analog **22** compared to **18** (~40-fold) may have been caused by the polar *N*-4 atom of the isoxazole forming an unfavorable interaction with the lipophilic phenyl ring, serving to destabilize the U-shaped binding conformation. Perhaps for a similar reason oxadiazole **26** was less potent than **1**.

In addition to the need for a hydrogen bond acceptor to interact with the backbone NH of Ala230 in AKT1, an additional hydrogen bond was required between the Glu228 backbone carbonyl and an appropriately positioned inhibitor hydrogen. The potent isoquinoline containing compound **9** provided an aryl CH:O interaction via isoquinoline H-1 and met these requirements. Additional analogs were prepared to examine AKT1 potency and selectivity (Table 2). The 3-aminoisoquinoline analog **27** was designed to form a hydrogen bond with the Ala230 backbone carbonyl, however, this added interaction did not appear to improve potency as **27** was 2–3-fold less potent than **9**. One potential explanation for this loss of potency is the desolvation

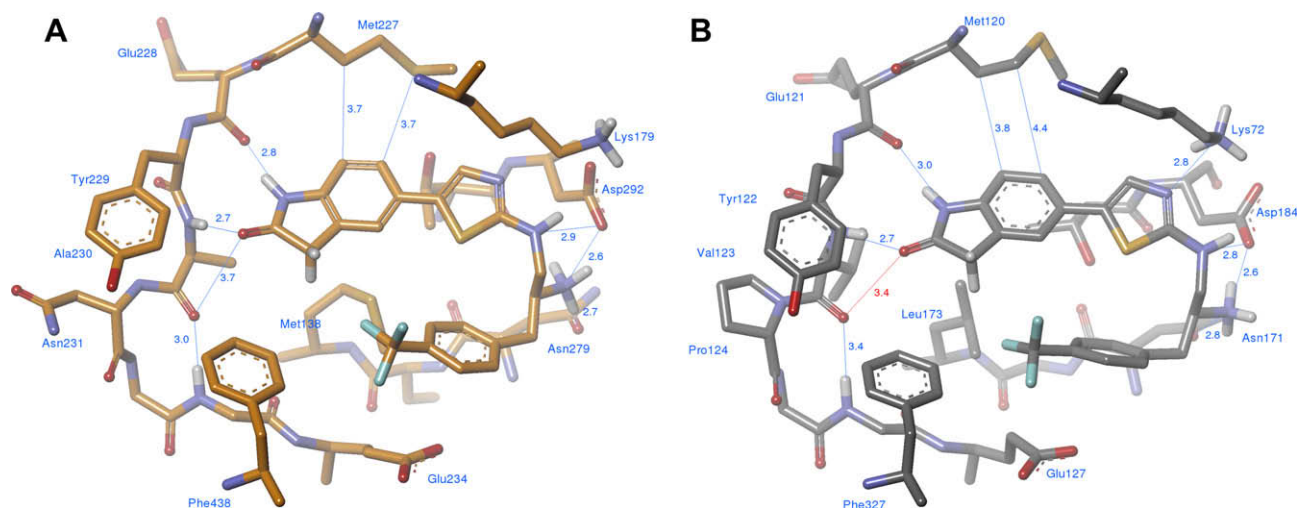


**Figure 2.** (A) Compound **36** modeled into AKT1 (PDB 3CQU6)<sup>17</sup> and (B) co-crystallized with PKA (PDB 3L9L).

**Table 2**

AKT, PKA and CDK2 enzyme inhibition and inhibition of PRAS40 phosphorylation in U-87 MG cells for thiazole-based linker strand binder analogs<sup>a</sup>

Compd	AKT1 IC <sub>50</sub> (nM)	PKA IC <sub>50</sub> (nM)	CDK2 IC <sub>50</sub> (nM)	pPRAS40 IC <sub>50</sub> (μM)
<b>9</b>	4.9 ± 3.6	5.9 ± 4.2	12.4 ± 5.7	0.43 ± 0.27
<b>27</b>	11.6 ± 0.7	8.6 ± 0.8	15.4 ± 5.4	0.89 ± 0.47
<b>28</b>	35 ± 18	126 ± 40	136 ± 22	1.3 ± 0.14
<b>29</b>	141 ± 4.8	489 ± 88	>2000	NT
<b>30</b>	613 ± 91	334 ± 88	>1000	NT
<b>31</b>	895 ± 226	230 ± 25	NT	NT
<b>32</b>	2406 ± 111	119 ± 1.0	>2000	NT
<b>33</b>	453 ± 63	417 ± 96	>2000	NT
<b>34<sup>b</sup></b>	8.5 ± 0.9	39.9 ± 8.5	NT	0.73 ± 0.35
<b>35</b>	77 ± 5.2	86.2 ± 7.4	55.3 ± 7.8	NT
<b>36</b>	18.3 ± 6.4	167 ± 50	185 ± 96	0.30 ± 0.08
<b>37</b>	8.0 ± 2.6	326 ± 118	138 ± 25	0.50 ± 0.35
<b>38<sup>c</sup></b>	27 ± 13	143 ± 71	285 ± 31	0.92 ± 0.58
<b>39</b>	15.4 ± 5.6	179	276	0.63, 0.64 <sup>c</sup>
<b>40</b>	3315 ± 284	2404 ± 1014	>25,000	NT
<b>41</b>	>1000	485	>1000	NT
<b>42</b>	>3000	>3000	>10,000	NT
<b>43</b>	95 ± 16	356 ± 39	>9000	6.0 ± 1.0

<sup>a</sup> Data is given as the mean ± standard deviation (SD) where three or more measurements were made. NT indicates not tested.

<sup>b</sup> 4-Chlorophenyl sidechain instead of 4-trifluoromethylphenyl sidechain.

<sup>c</sup> *n* = 2.

required for the second hydrogen of the anilinic amine. Similarly, quinazoline **28** placed its polar N1 atom in the same hydrophobic environment and was sixfold less potent than **9**. Compound **29**, containing the cinnoline linker binder, was nearly 30-fold less potent than **9** possibly due to an electrostatic repulsion between the Glu228 backbone carbonyl and the lone pair on the N1 of the cinnoline.

Benzazoles were also tested. The 6 substituted indazoles **30** and **31** had IC<sub>50</sub> values >600 nM, and may have formed a less than optimal hydrogen bond with Glu228. Although binding with geometry similar to isoquinoline, this loss of potency suggested the indazole H-3 was a less efficient aryl CH:O interaction donor than isoquinoline H-1. The incorporation of an amino group at the indazole 3 position was presumably too bulky and caused a further decline in potency in the case of the 6-yl substituted indazoles (**32**, IC<sub>50</sub> >2 μM). Benzisoxazole **33**, similar to **29**, did not satisfy Glu228. In contrast, the 5-yl substituted indazole analog **34** was >70-fold more potent than the corresponding 6-yl substituted indazole **30**. The 3-amino group of indazole **35** was designed to interact with the Ala230 backbone carbonyl, but the potency was ~9-fold less than the unsubstituted analog **34** (cf. **27** vs **9**).

Although trends toward more potent compounds were discovered throughazole ring and linker binder group modifications, selectivity and cellular activity remained a challenge. None of theazole core analogs in Table 1 nor the linker binder analogs **27–35** showed significant selectivity over PKA, and only **34** showed modest selectivity (PKA/AKT1 = 4.7). The isoquinoline, indazole and quinazoline analogs **9**, **18**, **27**, **28** and **34**, had significant and unfavorable cell shifts with cellular IC<sub>50</sub> values that were 37–95-fold higher than their IC<sub>50</sub> values in the enzyme assay.

Apart from aromatic linker strand binders, we also looked at non-aromatic compounds. It was anticipated that lactam analogs such as oxindole **36** could complement the hydrogen-bonding pattern of the linker strand. Indeed, **36** was reasonably potent (AKT1 IC<sub>50</sub> = 18 nM) and, interestingly, it was 9–10-fold selective over PKA and CDK2. Benzoxazolone **37**, benzothiazolone **38** and 3-methylbenzimidazolone **39** were similarly potent and selective. Dihydroquinolinone **40** was less potent (AKT1 IC<sub>50</sub> = 3315 nM) possibly due to increased repulsion from the Ala230 carbonyl, and in **41** the required U-shaped binding conformation was probably disrupted by an unfavorable interaction between the phthalazine carbonyl and the sidechain phenyl ring. Monocyclic analog

**42** did not have the required conformational constraints and its  $IC_{50}$  was  $>3 \mu M$ . The isoindolin-1-one analog **43** had an  $IC_{50} = 94.6 \text{ nM}$ ,  $\sim 5$ -fold less active than **36**. In addition to improved selectivity, the lactam analogs **36–39**, and **43** showed reduced cell shifts compared to the indazole and isoquinoline analogs (16–63-fold). For example, although **36** was less potent in the enzyme assay compared to **1** (18.3 nM vs 3.2 nM), it had a smaller enzyme to cell shift and cellular potency of the two compounds was similar (**36**,  $IC_{50} = 0.30 \mu M$ ; **1**,  $IC_{50} = 0.25 \mu M$ ). Inhibition of U-87 MG cell viability was confirmed for **36** ( $IC_{50} = 0.63 \mu M$ ).<sup>16</sup>

Compound **36** was modeled into the active site of AKT1<sup>17</sup> using a previously described hierarchical method,<sup>18</sup> and was also co-crystallized in PKA (Fig. 2). Similar to the previously described compounds,<sup>9</sup> **36** bound in a U-shaped conformation, making the expected key interactions with the linker residue backbone amide (AKT1, Ala230; PKA, Val123) and linker-2 glutamate carbonyl (AKT1, Glu228; PKA, Glu121). The improved selectivity of compound **36** relative to **9** may be explained in part by the smaller size of the linker-strand binder. As discussed in the previous Letter, the oxindole of **36** may have formed better hydrophobic interactions with the AKT1 floor residue (Met281) than with the PKA floor residue (Leu173).<sup>9</sup> Alternatively, this improved selectivity profile may also be explained by different linker residues in AKT versus PKA. Asparagine in AKT (Asn231) would likely allow greater flexibility of the AKT linker strand compared to PKA which contains a proline residue (Pro124) in this position. This flexibility may allow the AKT1 linker strand to relax in order to avoid a repulsive electrostatic interaction between the inhibitor carbonyl and the Ala230 backbone carbonyl, whereas PKA could not. Consequently an unfavorable electrostatic interaction in PKA (3.4 Å vs 3.7 Å) would reduce the potency of the lactam-based inhibitors on PKA, thereby improving selectivity.

Compounds **9**, **36** and **37** were advanced into in vivo experiments (Table 3). In rat pharmacokinetic (PK) studies, isoquinoline compound **9** was found to be cleared at a high rate and had moderate bioavailability. Oxindole compound **36** had lower clearance

than **9** and achieved higher exposures following oral dosing at 5 mg/kg. Benzoxazole **37** had poor bioavailability and low oral exposure. It was subsequently confirmed that compounds **36** and **37** were cleared via hepatic oxidation of the thiazole ring.<sup>19</sup> Based on rat PK data, compounds **9** and **36** were selected for in vivo pharmacodynamic (PD) studies in mice, measuring inhibition of hepatocyte growth factor (HGF) induced PRAS40 phosphorylation in the liver.<sup>20</sup> Six hours after a 30 mg/kg dose, **9** achieved a plasma concentration 1.7-fold above its cellular  $IC_{50}$ , and showed minimal inhibition of PRAS40 phosphorylation in vivo. In contrast, plasma concentration of **36** 6 h post dose was about 10-fold over its cellular  $IC_{50}$ , and significant inhibition of PRAS40 phosphorylation was observed (43%).

We next tested compound **36** in an in vivo tumor xenograft model. Accordingly, **36** was administered for 18 days to nude mice bearing U-87 MG tumors (15, 30, 60 mg/kg qd po).<sup>21</sup> Significant inhibition of tumor growth (93%) was observed at the 30 mg/kg dose relative to vehicle treated control. Although measured at different time-points, plasma exposures appeared to be similar in the efficacy study and the single dose PD experiment. Tumor growth and body weight data are shown in Figure 3. Tumor growth inhibition was dose proportional and treatment was tolerated with 2–10% loss in body weight over the course of the study compared to a gain of 2% for vehicle. In a screening panel of 43 kinases, compound **36** had  $IC_{50}$  values  $<500 \text{ nM}$  on 15 of these targets, including kinases that are involved in tumor growth regulation (e.g.,  $IC_{50}$  values: KDR, 0.30  $\mu M$ ; c-KIT, 0.11  $\mu M$ ; CDK1, 0.25  $\mu M$ ). Thus at the high plasma concentrations achieved during the tumor growth inhibition study, inhibition of other kinases may have contributed to the efficacy observed.

Flexible and convergent syntheses have generated a series of thiazole-based inhibitors of AKT. We have optimized compounds for potency on AKT and have demonstrated modest selectivity against PKA and CDK2 kinases. Inhibition of the phosphorylation of one AKT substrate, PRAS40, was demonstrated in U-87 MG cell culture and in a mouse liver PD model using **36**. Inhibition of

**Table 3**  
In vivo rat pharmacokinetic parameters, mouse liver PD effect and U-87 MG xenograft growth inhibition

Compd	Rat pharmacokinetic parameters						Mouse liver PD at 6 h		U-87 MG xenograft growth inhibition <sup>d</sup> (%)	Xenograft plasma concentration 3 h post last dose
	$t_{1/2}$ <sup>a</sup> (h)	CL <sup>a</sup> (L/h/kg)	V <sub>ss</sub> <sup>a</sup> (L/kg)	% F <sup>b</sup>	C <sub>max</sub> <sup>b</sup> (ng/mL)	AUC <sub>(0–24h)</sub> <sup>b</sup> (ngh/mL)	pPRAS40 (Thr246, %) <sup>c</sup>	Plasma concd ( $\mu M$ )		
<b>9</b>	2.9	2.7	7.1	20	66	387	4	1.5	NT	NT
<b>36</b>	4.3	1.0	6.8	64	417	2600	43*	3.5	93**	6.2 $\mu M$
<b>37</b>	3.8	1.6	6.7	11	68	348	NT	NT	NT	NT

<sup>a</sup> Dosing was 2 mg/kg iv in DMSO in  $n = 3$  male Sprague Dawley rats.

<sup>b</sup> Dosing was 5 mg/kg po in 2% HPMC, 1% Tween 80, pH 2 in  $n = 3$  male Sprague Dawley rats.

<sup>c</sup> Dosing was 30 mg/kg po in 0.1% PBS/BSA in  $n = 3$  female mice, \* $p = 0.0079$ . NT indicates not tested.

<sup>d</sup> Dosing was 18 d 30 mg/kg po in female CD1 nude mice ( $n = 10$ ), \*\* $p < 0.0001$ . NT indicates not tested.

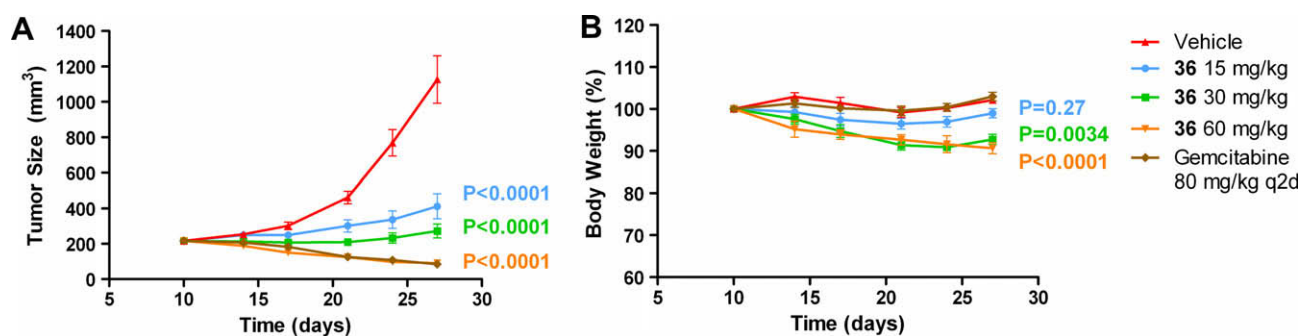


**Figure 3.** Compound **36** inhibited U-87 MG xenograft growth in CD1 nude mice with daily dosing over 18 d. (A) Tumor growth; (B) body weight normalized to day 1.

PRAS40 phosphorylation in vivo coincided with inhibition of xenograft tumor growth, albeit at high plasma concentrations where inhibition of off-target kinases involved in cell proliferation or regulation may have contributed to tumor growth inhibition. As AKT remains an attractive anti-cancer target, AKT inhibitors such as the ones presented here may be important for further development.

## References and notes

1. Hennessy, B. T.; Smith, D. L.; Ram, P. T.; Lu, Y.; Mills, G. B. *Nat. Rev. Drug Discovery* **2005**, *4*, 988.
2. Bader, A. G.; Khang, S.; Zhao, L.; Vogt, P. K. *Nat. Rev. Cancer* **2005**, *5*, 921.
3. Testa, J. R.; Bellacosa, A. *Proc. Natl. Acad. Sci. U.S.A.* **2001**, *98*, 10983.
4. (a) Cully, M.; You, H.; Levine, A. J.; Mak, T. W. *Nat. Rev. Cancer* **2006**, *6*, 184; (b) Leslie, N. R.; Downes, C. P. *Biochem. J.* **2004**, *382*, 1.
5. Tokunaga, E.; Kimura, Y.; Oki, E.; Ueda, N.; Futatsugi, M.; Mashino, K.; Yamamoto, M.; Ikebe, M.; Kakeji, Y.; Baba, H.; Maehara, Y. *Int. J. Cancer* **2006**, *118*, 284.
6. Altomare, D. A.; Testa, J. R. *Oncogene* **2005**, *24*, 7455.
7. Lindsley, C. W.; Barnett, S. F.; Layton, M. E.; Bilodeau, M. T. *Curr. Cancer Drug Target* **2008**, *8*, 7.
8. (a) ClinicalTrials.gov identifier NCT00920257.; (b) Tolcher, A. W.; Yap, T. A.; Fearen, I.; Taylor, A.; Carpenter, C.; Brunetto, A. T.; Beeram, M.; Papadopoulos, K.; Yan, L.; de Bono, J. J. *Clin. Oncol.* **2009**, *27*, 15s.
9. Zeng, Q.; Bourbeau, M. P.; Wohlhieter, G. E.; Yao, G.; Monenschein, H.; Rider, J. T.; Lee, M. R.; Zhang, S.; Lofgren, J. A.; Freeman, D. J.; Li, C.; Tominey, E.; Huang, X.; Hoffman, D.; Yamane, H.; Tasker, A. S.; Dominguez, C.; Viswanadhan, V. N.; Hungate, R.; Zhang, X. *Bioorg. Med. Chem. Lett.* **2010**, *20*, 1652.
10. U-87 MG cells in 5% FBS were incubated with inhibitors in threefold serial dilutions for 1 h at 37 °C. The cells were lysed and PRAS40 phosphorylation was quantified by ELISA assay. pPRAS40 was normalized to total PRAS40.
11. Posakony, J. J.; Grierson, J. R.; Tewsonin, T. J. *J. Org. Chem.* **2002**, *67*, 5164.
12. (a) Hauske, J. R.; Dorff, P.; Julin, S.; Martinelli, G.; Bussolari, J. *Tetrahedron Lett.* **1992**, *33*, 3715; (b) Brown, D. G.; Velthuisen, E. J.; Commerford, J. R.; Brisbois, R. G.; Hoye, T. R. *J. Org. Chem.* **1996**, *61*, 2540.
13. Smrcina, M.; Majer, P.; Majerova, E.; Guerassina, T. A.; Eissenstat, M. A. *Tetrahedron* **1997**, *53*, 12867.
14. Guram, A. S.; King, A. O.; Allen, J. G.; Wang, X.; Schenkel, L. B.; Chan, J.; Bunel, E. E.; Faul, M. M.; Larsen, R. D.; Martinelli, M. J.; Reider, P. J. *Org. Lett.* **2006**, *8*, 1787.
15. Ishiyama, T.; Murata, M.; Miyaura, N. *J. Org. Chem.* **1995**, *60*, 7508.
16. U-87 MG cells were seeded on a 96-well cell culture plate at 6000 cells/well in 5% FBS, and treated with **36** in threefold serial dilutions for three days. Cell viability was measured by alamarBlue cell staining (Invitrogen, DAL1100).
17. Lippa, B.; Pan, G.; Corbett, M.; Li, C.; Kauffman, G. S.; Pandit, J.; Robinson, S.; Wei, L.; Kozina, E.; Marr, E. S.; Borzillo, G.; Knauth, E.; Barbacci-Tobin, E. G.; Vincent, P.; Troutman, M.; Baker, D.; Rajamohan, F.; Kakar, S.; Clark, T.; Morris, J. *Bioorg. Med. Chem. Lett.* **2008**, *18*, 3359.
18. Lee, M. R.; Sun, Y. J. *Chem. Theor. Comp.* **2007**, *3*, 1106.
19. Subramanian, R.; Lee, M. R.; Allen, J. G.; Bourbeau, M. P.; Fotsch, C.; Hong, F.-T.; Tadesse, S.; Yao, G.; Yuan, C. C.; Surapaneni, S.; Skiles, G. L.; Wang, X.; Wohlhieter, G. E.; Zeng, Q.; Zhou, Y.; Zhu, S.; Li, C. *Chem. Res. Toxicol.* **2010**, doi:10.1021/tx900414g.
20. Mice ( $n = 3$ ) were dosed with compounds **9** or **36** (30 mg/kg po) and after 6 h, AKT signaling was stimulated in mouse liver by treatment with HGF via tail vein injection. Five minutes post-HGF treatment, the mice were sacrificed and livers were harvested for quantitation of phospho- and total PRAS40 by ELISA. pPRAS40 was normalized to total PRAS40 to calculate inhibition. Factorial ANOVA followed by Dunnett's post hoc test was used to determine statistical significance. Data for **36** was from one of two experiments.
21. 10-Week-old female CD1 nude mice (Charles River Laboratories, Wilmington, MA) were injected sc in the flank with  $5 \times 10^6$  U-87 MG cells in 0.2 mL DMEM. On day 10, mice were randomized into groups of  $n = 10$  with an initial tumor volume of  $\sim 200$  mm<sup>3</sup>. Diet was supplemented. Tumor measurements and body weights were recorded twice per week. Tumor volume was calculated as length  $\times$  width  $\times$  height. Tumor measurements were analyzed by RMANOVA using StatView version 5.0.1 (SAS Institute, Cary, NC). Scheffé's post hoc test was used to determine statistical significance. Data for **36** was from one of three experiments.